Int. J. Heat Mass Transfer. Vol. 15, pp. 1865–1886. Pergamon Press 1972. Printed in Great Britain

THERMODYNAMIC ANOMALIES NEAR THE CRITICAL POINT OF STEAM*

J. M. H. LEVELT SENGERS and SANDRA C. GREER

Institute for Basic Standards, National Bureau of Standards, Washington, D.C., U.S.A.

(*Received* 21 *June* 1968 *and in revised form* 7 *December* 1971)

Abstract—Ideas about the character of critical anomalies obtained from the lattice gas model are tested on the thermodynamic properties of steam, using methods developed for nonpolar gases. The critical anomalies in steam are shown to be nonclassical and very similar to those of simple gases. Specifically, the exponents obtained by power-law analysis of the coexistence curve, specific heat C_v and compressibility K_T are $\beta = 0{\cdot}347 \pm 0{\cdot}005$, $\alpha = 0{\cdot}1 \pm 0{\cdot}05$, $\gamma = 1{\cdot}20 \pm 0{\cdot}05$, implying $\delta = 4{\cdot}45$. Since the critical point is thus a point of nonanalyticity in the thermodynamic behavior, the scaled equation of state may be an appropriate means to describe the critical region. Some results of such a scaled analysis of the PVT data are presented and shown to be consistent with independently measured vapor pressure and specific heat data and with the exponents quoted. The best value obtained for the critical temperature by scaling is 373·9°C ± 0·05°, values between 0·322 and 0·327 g/cm^3 are obtained for the critical density depending on the property analyzed.

NOMENCLATURE

- P, pressure;
- V, volume;
- A, Helmholtz free energy;
- a, A/V, Helmholtz free energy per unit volume;
- μ, chemical potential;
- T, temperature;
- T_c, critical temperature;
- ΔT, reduced temperature difference $(T - T_c)/T_c$;
- ρ, N/V, density;
- ρ_c, critical density;
- ρ_L, liquid density;
- ρ_G, gas density,
- $\bar{\rho}$, rectilinear diameter density;
- $\Delta\rho$, reduced density difference $(\rho - \rho_c)/\rho_c$, $T > T_c$; $(\rho - \bar{\rho})/\rho_c$, $T < T_s$;
- K_T, isothermal compressibility $(1/\rho)(\partial\rho/\partial P)_T$;
- C_v, specific heat at constant volume;
- C_{vi}, internal specific heat (C_v minus perfect gas contribution);
- C_v/V, constant volume heat capacity density;
- $\alpha, \beta, \gamma, \delta$, exponents of anomalies in specific heat, coexistence curve, compressibility and critical isotherm, resp.

1. INTRODUCTION

AMONGST the requirements a good equation-of-state has to fulfil are the following: the equation must fit to within experimental accuracy the data considered reliable; and thermodynamic properties derived from the equation must agree with directly measured values.

Both requirements are hard to satisfy in the critical region. Not only is it difficult to represent the PVT data by an equation-of-state, but also, even when an equation satisfactorily describing the experimental data has been found, other thermodynamic properties derived from it usually deviate systematically from independently measured data. A typical example of this state of affairs are the N. E. L. Steam Tables [1] where tabulated entropy and enthalpy values, derived from the equation-of-state, had to be supplemented by correction tables describing the deviation of the calculated quantities from

* Presented at the 7th International Conference on Properties of Steam, Tokyo, Japan, September 1968.

experiment. It need not be stressed that inconsistencies of this type are undesirable.

The insight into the nature of the critical point that has been gained in recent years has made clear why the critical region presents such a stubborn problem. The reason is that the critical point, in most instances, has a non-analytical character; that is, the Helmholtz free energy cannot be expanded in powers of density and temperature at the critical point [2]. Indirectly, this has been known since the early 1900's. Van Laar [3] proved that the existence of a Taylor expansion implies that the coexistence curve is of the 2nd or the 4th degree, while it was well known at that time that these curves are approximately cubic [4]. Direct experimental evidence for nonanalyticity is the divergence of the specific heat at constant volume, observed for a variety of gases such as He [5], Ar [6], Xe and CO_2 [7], O_2 and N_2 [6]. This implies that $(\partial^2 A/\partial T^2)_V$ is infinite for these gases at the critical point, thus, precluding a Taylor expansion of the free energy. Equations-of-state used in engineering applications are almost always analytic at the critical point. Consequently, an excessive number of terms and adjustable constants is needed to fit the data within experimental accuracy, whereas thermal properties derived from the equation cannot represent the experimentally observed anomalies.

The non-analyticity of critical behavior is closely connected with the fact that on approaching the critical point, correlations in the system extend far beyond the range of the intermolecular forces; this causes the critical phenomenon to be highly independent of the detailed character of the interaction forces so that critical phenomena in different systems are closely analogous [2]. On the other hand, for systems with intermolecular forces of such long range that correlations never extend beyond this range, one should expect classical behavior [8] as exemplified in van der Waals' equation which is analytic at the critical point. Some ferroelectrics show such classical behavior near their Curie points.

These considerations lead us to steam as a particularly interesting substance. In contrast to most other fluids, where the interaction forces are van der Waals forces with a $1/r^6$ range of potential, a substantial part of the interaction in steam is due to the dipole potential that falls off as $1/r^3$. Thus it is of interest to investigate whether the behavior of steam in the critical region is analogous to that of other fluids. If so, a reappraisal of the equation-of-state of steam near the critical point in the light of the recent insights into critical anomalies is mandatory.

In this paper the nature of critical behavior in models with long- and with short-range forces will be briefly summarized. Next, a short survey will be given of the critical anomalies found in nonpolar fluids like He, CO_2 and others. Then, the character of the critical region of steam will be analyzed using the techniques developed for normal fluids. The critical region of steam will be shown to be quite analogous so that of nonpolar substances, and therefore nonanalytic at the critical point. Some suggestions for a new approach to the description of the critical region of steam will then be offered.

2. CRITICAL ANOMALIES IN CLASSICAL AND NONCLASSICAL MODEL SYSTEMS AND IN REAL FLUIDS

Two mathematical models provide the guidelines for describing critical anomalies. The first, van der Waals' equation, is an example of the classical (analytic) inner field theories in which long-range forces between molecules are implicitly assumed [8]. The Ising model, on the other hand, a lattice model with nearest-neighbor interactions only, shows non-classical (non-analytic) behavior. The latter becomes a model for the gas–liquid transition, the so-called lattice gas [9], if molecules and empty sites are distributed over the lattice and an attractive energy is assigned to pairs of molecules occupying adjacent sites. In both models, the critical behavior of thermodynamic properties is characterized by power laws describing the asymptotic mathematical behavior. Thus, for classical equations like that of van der Waals, in which only

the lowest two derivatives of pressure with respect to volume vanish, these power laws are the following [2, 3, 10, 11]. The top of the coexistence curve is quadratic, hence

$$V_L - V_G \sim \rho_L - \rho_G \sim (T_c - T)^{\beta} \qquad (1)$$

with $\beta = \frac{1}{2}$.

The critical isotherm is of the third degree, so that

$$P - P_c \sim (V - V_c)^{\delta} \sim (\rho - \rho_c)^{\delta} \qquad (2)$$

with $\delta = 3$.

Since the chemical potential μ is related to the pressure by $N\mathrm{d}\mu = V\mathrm{d}P - S\mathrm{d}T$, it follows that along the critical isotherm, the asymptotic behavior of μ is the same as that of P, namely

$$\mu - \mu_c \sim (V - V_c)^{\delta} \sim (\rho - \rho_c)^{\delta} \qquad (3)$$

with $\delta = 3$.

The compressibility K_T on the critical isochore goes to infinity inversely proportional to $T - T_c$,

$$K_T = -\left(\frac{1}{V}\right)\left(\frac{\partial V}{\partial P}\right)_T = \rho^{-2}\left(\frac{\partial \rho}{\partial \mu}\right)_T \sim (T - T_c)^{-\gamma} \qquad (4)$$

with $\gamma = 1$.

In the one-phase region near the phase boundary the compressibility of the gas is higher than that of the liquid but they both diverge in the same way, again as $|T - T_c|^{-\gamma}$ with $\gamma = 1$. Likewise, the quantity $\partial\mu/\partial\rho = 1/(\rho^2 K_T)$ goes to zero as $|T - T_c|^{\gamma}$ with $\gamma = 1$, along the critical isochore and along the phase boundary. The specific heat at constant volume C_{vi} on the critical isochore below T_c rises to a finite limit at the critical point and then falls off to a lower value in the one-phase region.

This critical behavior of the classical equation is to be contrasted with that of the non-classical three-dimensional Ising model [12]. For this, the top of the coexistence curve is close to cubic, $\beta = 0{\cdot}3125$. The critical isotherm is of a degree close to 5, $\delta = 5{\cdot}0$. The compressibility diverges faster than in the classical case, with $\gamma = 1{\cdot}25$. The internal specific heat at constant volume C_{vi} diverges a little faster than logarithmic, both above and below T_c, $C_{vi} \sim |T - T_c|^{-\alpha}$ with $\alpha = 0{\cdot}125$.

The critical exponents α, β, γ, δ are not free to assume just any values independently. Thermodynamic considerations require that the following relations be obeyed [13]:

$$\beta(\delta + 1) \geqslant 2 - \alpha$$

$$\gamma + 2\beta \geqslant 2 - \alpha. \qquad (5)$$

It is readily seen that the exponents of the classical case and of the Ising model fulfil the relations (5) with the equal sign.

Power-law analyses of experimental data for a number of non-polar fluids such as He^3, He^4, Ar, Xe, and O_2 [14–17], reveal the following picture. The top of the coexistence curve is near cubic, $\beta = 0{\cdot}34$–$0{\cdot}36$. The degree δ of the critical isotherm is between 4·0 and 4·6. The compressibility exponent γ is between 1·1 and 1·3, the specific heat exponent α between 0 and 0·15. Thus the exponents of real gases are much closer to those of the Ising model than to those of classical theory. In addition, the exponents remain essentially the same from one gas to another, in accordance with the presence of long-range correlations, as mentioned above.

3. SYMMETRY

The analyticity of the classical equation of state has as a consequence that critical exponents and critical coefficients are the same whether one approaches the critical point from the low- or from the high-density side. Apart from this, there are in general no striking symmetries, and the loci of maximum compressibility, maximum C_v, etc., all move away from the critical isochore when one leaves the critical point (Fig. 1). The lattice-hole symmetry of the Ising model, on the other hand, entails a curious symmetry character, not apparent in the usual free energy $A(V, T)$ and pressure $P(V, T)$ coordinates, but revealed in the alternative ones free energy per unit volume $a(\rho, T)$ and chemical potential $\mu(\rho, T)$. The coexistence curve and configurational free energy per unit volume are both symmetric

with respect to the critical density, whereas the chemical potential is antisymmetric in density with respect to its value on the critical isochore (Fig. 1). Consequently, the quantity $\rho^2 K_T = (\partial\rho/\partial\mu)_T$ is again symmetric with respect to the critical density, and so is the internal

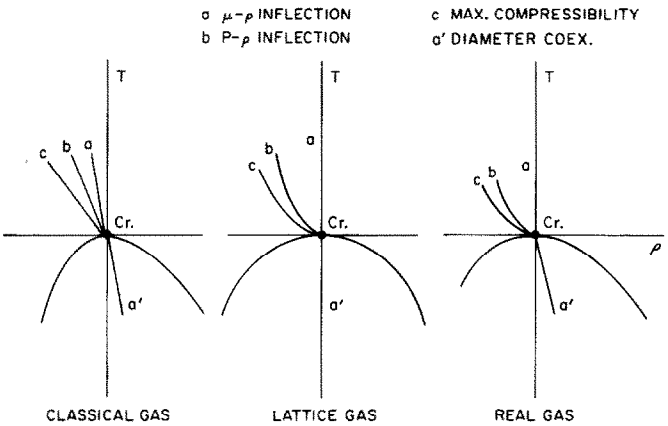

FIG. 1. Symmetry character of the critical region of gases in the temperature–density plane.

specific heat per unit volume C_{vi}/V. Moreover, since μ is regular everywhere in the one-phase region, its antisymmetry implies that it is regular along the critical isochore [19], in contrast to the classical equation for which $\partial^2\mu/\partial T^2$ is discontinuous at the critical point. In the lattice gas, pressure, compressibility and specific heat do not have any natural symmetry character.

Real gases, exhibiting non-analytic critical behavior but lacking the Ising model particle-hole symmetry, cannot be expected, *a priori*, to possess any of the symmetries discussed above. However, experimentally it has been established not only that exponents and coefficients are the same on the low and high density sides of the critical isochore [18] but also that the μ–ρ isotherms show anti-symmetry with respect to this isochore over wide temperature ranges, for densities within 25 per cent from critical [15, 19] (Fig. 1). Likewise, experimental values of $\rho^2 K_T$ on the two sides of the coexistence curve show a measure of symmetry [15, 16]. Neither the specific heat itself, nor the quantity C_{vi}/V shows a particular symmetry. However, combining the thermodynamic relation

$$\frac{C_v}{V} - \frac{C_{v_c}}{V_c} = \int_{\rho_c}^{\rho} -T\left(\frac{\partial^2\mu}{\partial T^2}\right)_\rho d\rho \qquad (6)$$

and the observed antisymmetry of the $\mu(\rho)$ relation we conclude that the combination

$$\frac{C_v}{V} + T\rho\left(\frac{\partial^2\mu}{\partial T^2}\right)_{\rho_c}$$

must be symmetric with respect to the critical isochore. $(\partial^2\mu/\partial T^2)\ \rho_s$ is, however, experimentally inaccessible except in the two-phase region where it is obtained from the volume dependence of C_v by the relation [20]

$$\frac{C_v}{VT} = \left(\frac{\partial^2\rho}{\partial T^2}\right)_v - \rho\left(\frac{\partial^2\mu}{\partial T^2}\right)_v. \qquad (7)$$

In the one-phase region it has been possible in a

number of cases [5, 19] to symmetrize C_v/V by adding a part linear in the density, thus obtaining an estimate of $(\partial^2\mu/\partial T^2)\rho_c$. So far there has been no experimental evidence that this quantity is anomalous near the critical point, in contrast to classical behavior but in agreement with the Ising model. We conclude that asymptotically near the critical point real gases exhibit the same symmetry as the Ising model.

4. THE SCALING LAWS

In an attempt to summarize the observed asymptotic power laws and symmetries in an equation of state, Widom first formulated the so-called scaling laws for the critical region of fluids [21]. In Griffiths' reformulation [22] these become:

$$\frac{\Delta\mu}{\Delta\rho|\Delta\rho|^{\delta-1}} = h(x) \tag{8}$$

with

$$x = \Delta T/|\Delta\rho|^{1/\beta}$$

where

$$\Delta\mu = [\mu(\rho, T) - \mu(\rho_c, T)]/P_cV_c$$

$$\Delta\rho = (\rho - \rho_c)/\rho_c$$

$$\Delta T = (T - T_c)/T_c.$$

Thus, chemical potential differences $\Delta\mu$, when scaled by $\Delta\rho|\Delta\rho|^{\delta-1}$, are functions of one variable only, the scaled temperature $x = \Delta T/|\Delta\rho|^{1/\beta}$. The function $h(x)$ is not specified, but has to fulfil a number of mathematical conditions [22]. These follow from thermodynamic stability requirements and from the condition that μ be free of anomalies inside the entire one-phase region. For details see [19, 22] and the Appendix. It can be shown [21, 22] that all power laws are incorporated in (8) and that the relations (5) between the exponents hold with the equality sign.

For a number of simple fluids, like He^3 [15] and He^4, CO_2 and Xe [19] the chemical potential has been shown to scale in the critical region. We shall investigate this point for steam in Sec. 9.

One should realize that the scaled equation (8) does not give a complete description of thermodynamic behavior. Since it is not a fundamental equation, an unknown temperature-dependent integration constant will appear in the free energy. Moreover, the quantity $\mu(\rho_c T)$ has been left unspecified and will have to be obtained from experiment somehow. (See Sec. 3 and the Appendix.)

5. THE COEXISTENCE CURVE OF STEAM. THE EXPONENT β

We proceed to deduce the character of the critical anomalies in steam from experimental data in the critical region. In all cases the raw data will be studied rather than smoothed or tabulated data derived from them; correlating techniques used in tabulation are generally analytic and, being possibly at odds with the analytic character of the data in this respect, could introduce an undesirable bias. The critical point of steam occurs, roughly speaking, at 374°C, a density of 0·3 g/cm^3 and a pressure of 220 bars. The critical pressure and temperature are much higher than for most other gases of low molecular weight. Because of its practical importance, the critical region has been widely explored even though it is not very accessible experimentally.

The first property to be studied here is the coexistence curve. This curve has been measured directly by Eck [23] who observed the temperatures of meniscus disappearance for samples at various known overall densities. The samples were contained in quartz tubes. Gas and liquid densities were not obtained at coexistence and thus some assumption about the behavior of the average density has to be made before the data can be analyzed. If coexisting densities are interpolated on a large-scale plot, it is found that the curve of average density is straight within error (Fig. 2). This straight line, called the rectilinear diameter, can be described with

$$\bar{\rho} \equiv (\rho_L + \rho_G)/2 = [1 + a(T - T_c)/T_c]\,\rho_c,$$

where

$$\rho_c = 0{\cdot}325 \text{ g/cm}^3 \text{ and } a = 1{\cdot}5.$$

Several correlations for steam [24–26] show curvature of the diameter near T_c and, consequently, rather different values for ρ_c, namely 0·305 [24], 0·318 [25] and 0·315 [26]. We will present independent evidence for a high value of ρ_c later. However, here we wish to point out that recent theoretical developments strongly suggest that the diameter is not straight, but, rather, that its temperature derivative diverges weakly at the critical point, at least as fast as does the specific heat [27]. On the other hand, theoretical estimates of the effect, based on model calculations, indicate that the curvature may be too small to be detected [28]. Also, significant deviations from the law of the rectilinear diameter have not been detected in the best experimental data available for other substances [15, 16, 18]. In our analysis we will use the law of the rectilinear diameter, but will explore the effect of using a curved diameter of the form suggested theoretically. In other words, we shall attempt to fit the data with the expressions

$$\Delta\rho = B|\Delta T|^{\beta}$$

with

$$\Delta\rho = (\rho - \bar{\rho})/\rho_c, \quad \Delta T = (T - T_c)/T_c,$$

$$\bar{\rho} = (\rho_L + \rho_G)/2 \tag{9}$$

and

$$\bar{\rho} = \rho_c[1 + a_0\Delta T] \quad \text{(rectilinear diameter)} \tag{10}$$

or

$$\bar{\rho} = [1 + a_\alpha(\Delta T)^{1-\alpha}] \text{(curved diameter)}. \tag{11}$$

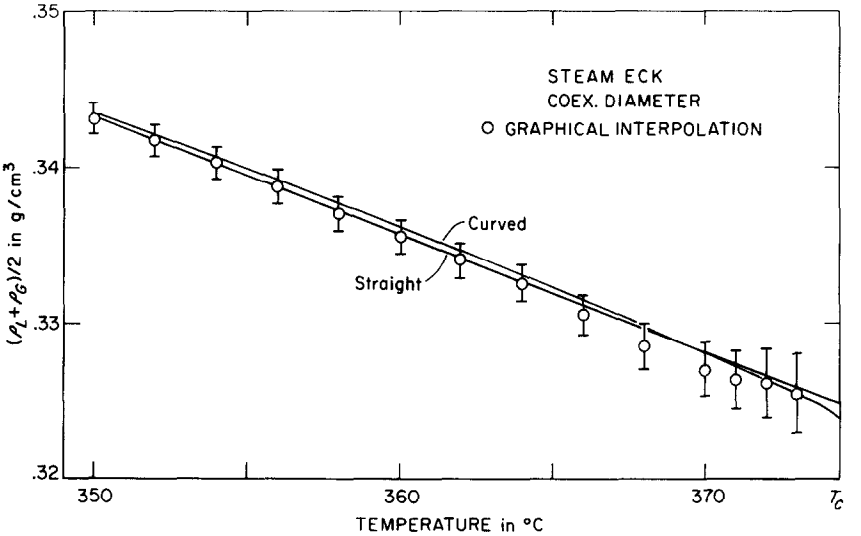

FIG. 2. Values of the average coexisting densities of steam, $\bar{\rho} = (\rho_L + \rho_G)/2$, versus temperature, obtained graphically. The straight line (10) fits these data about as well as the curved one, (11), with $\alpha = 0{\cdot}1$.

In fitting with these equations, ρ_c, T_c, β, B, a (and α) have to be considered adjustable parameters. A linear least-squares fit of $\ln(\Delta\rho)$ vs. $\ln(\Delta T)$ is performed, while T_c, β and ρ_c are varied in steps. The data points are given weights assuming constant standard errors, $\sigma_\rho = 0{\cdot}001$ g/cm^3 and $\sigma_T = 0{\cdot}01$°C, respectively, in density and temperature. The variance of $\ln(\Delta\rho)$ due to errors in density is then equal to $[\sigma_\rho\rho_c/(\Delta\rho)]^2$, and, by propagation of errors and using (9), its variance due to temperature error is $[\beta\sigma_T/T_c(\Delta T)]^2$. Since errors in density and temperature are uncorrelated, the variances can be added and a weight

$$w_i = \{[(\sigma_\rho/\rho_c(\Delta\rho)]^2 + [\beta\sigma_T/T_c(\Delta T)]^2\}^{-1}$$

is assigned to each data point. These estimates of the absolute error are not far off the mark, the standard deviation of the best fit turning out only slightly larger than unity.

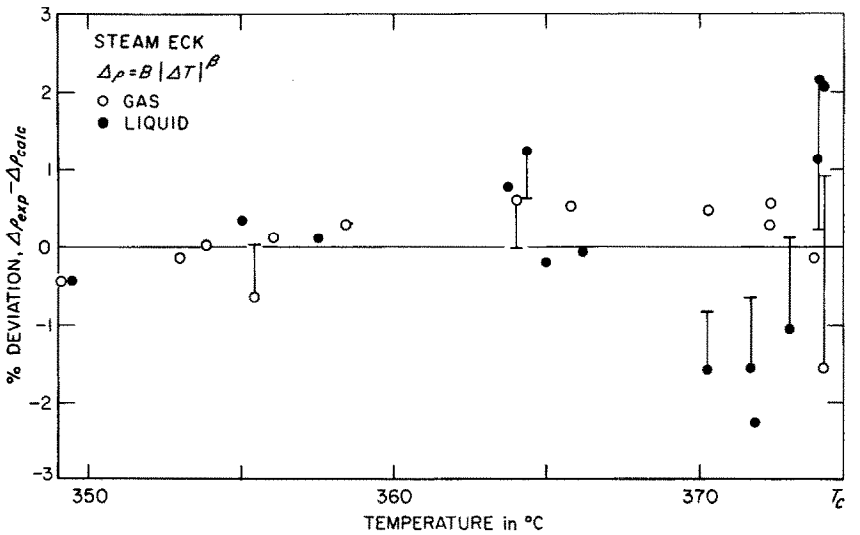

FIG. 3. Percentage deviations of the experimental reduced density differences, $\Delta\rho = (\rho - \bar{\rho})/\rho_s$, from the ones calculated according to (12), plotted vs. temperature along the coexistence curve of steam.

The data point at 374·17°C was omitted from the fit since density gradients must be present in a cell 6 cm high this close to the critical temperature. The other 27 points were fitted by varying the values of T_c, ρ_c and a in steps. The fit with the lowest standard deviation, $\sigma = 1{\cdot}11$, yielded the following results:

$$\begin{aligned} T_c &= 374{\cdot}33°\text{C} \\ \rho_c &= 0{\cdot}325\ \text{g/cm}^3 \qquad B = 2{\cdot}240 \\ a &= 1{\cdot}5 \qquad\qquad \beta = 0{\cdot}3505 \end{aligned} \tag{12}$$

The deviations of the experimental points from the fitted curve are shown in Fig. 3. Most data points are fitted within 2 standard deviations. A variety of parameter combinations has been found to fit the data almost as well as the set (12). Some examples are shown in Table 1. Although there is, therefore, some latitude in the assignment of values to ρ_c, T_c, a, etc., the unequivocal result is obtained that β is close to 0·35, a non-classical value not significantly different from values obtained for other substances [16–18].

Table 1. Least-squares fits to the coexistence curve of steam, Eck's data [23]

	Standard deviation of fit (9)	T_c(°C)	ρ_c(g/cm^3)	Coefficient of diameter (10) or (11)	β
Straight diameter	1·11	374·33	0·325	1·5	0·3505
	1·19	374·35	0·324	1·6	0·3519
	1·17	374·35	0·324	1·65	0·3522
	1·25	374·35	0·325	1·60	0·3534
	1·27	374·30	0·324	1·65	0·3465
	1·66	374·25	0·324	1·60	0·3403
Curved diameter	1·15	374·35	0·324	1·15	0·3525
	1·26	374·35	0·324	1·20	0·3529
	1·32	374·35	0·325	1·10	0·3535
	1·66	374·25	0·324	1·15	0·3409

Several fits have been done with a curved diameter (11) assuming $\alpha = 0{\cdot}1$. The diameter is described about as well as by a straight line (Fig. 2). The best fit to (9) using (11) has a standard deviation of 1·15 and is obtained by the parameter combination $T_c = 374{\cdot}35°C$, $\rho_c = 0{\cdot}324$, $a = 1{\cdot}15$, while $\beta = 0{\cdot}3525$. Thus, the hypothesis of a curved diameter does not affect the estimates of the critical density and the exponent β significantly.

Optimum values for T_c are always near 374·35°C, in contrast to values between 374·21°C and 374·26°C reported by Eck by visual observation. However, the standard deviation of the fit is not very sensitive to the choice of T_c, although fits with the low T_c values are definitely less good (Table 1). Note that T_c choices in Eck's range correspond to β values near 0·34.

The Eck data have been criticized because of the presence of dissolved quartz. His high values of T_c (and the even higher ones found here) may perhaps be explained by the presence of such an impurity. However, we do not expect it to affect the value of β; impurity concentrations as high as 1 per cent have been shown to leave β unchanged in CO_2 and N_2O [18]. Also, theoretical estimates for impure Ising systems [29] indicate that only massive amounts of a second substance will modify β in an experimentally detectable way.

We now turn to a set of heat measurements on steam from which the coexistence curve can be constructed independently. We refer to the very precise latent heat measurements by Osborne, Stimson and Ginnings [30], OSG. By measuring the heat input into a steam sample maintained at constant temperature in the two-phase region while known amounts of gas or liquid were extracted, they obtained two latent-heat quantities which they called γ and β, but which we will relabel g and b to avoid confusion with critical exponents. These quantities are related to coexisting densities as follows:

$$b = (T/\rho_L)/(\mathrm{d}p/\mathrm{d}T)_{\mathrm{vap}},$$
$$g = (T/\rho_G)/(\mathrm{d}p/\mathrm{d}T)_{\mathrm{vap}}. \qquad (13)$$

It is possible to analyze the coexistence curve of steam without further knowledge of the vapor pressure. This is done as follows. From (13) it follows that

$$\frac{g-b}{g+b} = \frac{\rho_L - \rho_G}{\rho_L + \rho_G} = \frac{\rho_L - \rho_G}{2\rho_c(1 + a|\Delta T|)}. \qquad (14)$$

Thus the quantity

$$(1 + a|\Delta T|)\,(g-b)/(g+b)$$

equals $\Delta\rho$, the reduced coexisting density difference. These data are rather unique in that determinations were repeated at each measured pair b, T or g, T; thus the standard deviation of each mean value can be directly estimated and

Table 2. Least-squares fits of the coexistence curve of steam, OSG data [30]

T_c(°C)	s.d.	β	s.d.	β	s.d.	β	s.d.	β
Straight diameter coefficient a_0 (10) →	1·55		1·575		1·60		1·625	
373·87	1·99	0·3348	1·54	0·3357	1·16	0·3365	0·94	0·3374
373·86	1·53	0·3346	1·11	0·3355	0·81	0·3363	0·81	0·3371
373·85	1·13	0·3344	0·80	0·3353	**0·74**	**0·3361**	1·01	0·3369
373·84	0·91	0·3342	0·81	0·3350	1·03	0·3359	1·41	0·3367
373·83	1·00	0·3340	1·14	0·3348	1·48	0·3357	1·90	0·3365
Curved diameter coefficient a_z (11) →	1·40		1·425		1·45		1·475	
373·89	1·95	0·3408	1·47	0·3418	1·10	0·3429	0·95	0·3439
373·88	1·53	0·3406	1·10	0·3416	**0·88**	**0·3427**	1·00	0·3437
373·87	1·19	0·3404	0·91	0·3414	0·95	0·3425	1·29	0·3435
373·86	1·04	0·3402	1·01	0·3412	1·27	0·3422	1·71	0·3433
373·85	1·16	0·3400	1·35	0·3410	1·73	0·3420	2·19	0·3431

used to weigh $\ln\{(g-b)/(g+b)\}$. The standard deviation of the fit goes through a deep minimum when T_c and a are varied. Some samples are shown in Table 2. For the best fit, with s.d. = 0·74, the mean values of g and b, their s.d's, the estimated error of $\ln\Delta\rho$ and the deviations from the fitted curve are shown in Table 3.

6. THE COMPRESSIBILITY OF STEAM. THE EXPONENT γ

The exponent γ, as explained in Section 2, describes the limiting behavior of the compressibility K_T, and of the more desirable quantity $(\partial\mu/\partial\rho)_T = (\rho^2 K_T)^{-1}$ when the critical point is approached along the coexistence curve,

Table 3. OSG data [30], standard deviations of their means and of $\Delta\rho$, and residuals of best fit

T (°C)	g	$\sigma_{\bar{g}}$	b	$\sigma_{\bar{b}}$	Estimated s.d. of $\Delta\rho$, %	Residual of $\Delta\rho$, %
330	1295·35	0·064	155·92	0·047	0·0075	0·0007
350	1112·38	0·156	220·09	0·091	0·018	−0·0048
360	989·12	0·298	269·93	0·036	0·019	0·0002
365	909·51	0·47	305·30	0·48	0·12	0·0067
370	800·44	0·28	359·35	0·48	0·15	−0·068
372	733·65	0·69	395·48	0·21	0·16	0·18
373	683·05	0·54	427·56	0·65	0·35	−0·31
373·5	642·98	2·1	452·35	1·82	1·4	1·5
374	586·62	5·8	504·3	5·3		

$T_c = 373{\cdot}85$°C; reduced slope = 1·6; $\beta = 0{\cdot}3361$; $B = 2{\cdot}152$; $\Delta\rho \equiv (1 + a|\Delta T|)(g-b)/(g+b) = B|\Delta T|^{\beta}$.

In these fits, we have omitted the highest point at 374·00°C. First of all, the authors had great difficulty in measuring it. Secondly, recent experiments by Blank [31] indicate that the critical temperature is lower than the value obtained by us from Eck's data and, in fact, lower than 374°C. Thirdly, gravity effects alone would have caused an appreciable difference between densities at the top and the bottom of the calorimeter from which the samples were taken. For the OSG data, the optimum value of the critical temperature is 373·85°C, in good agreement with Blank's value of 373·91°C. The optimum value obtained for β is again definitely nonclassical, namely 0·336. However, it is rather low as compared to that from Eck's data and also lower than for other substances. On repeating the fit to the OSG data using a curved diameter rather than a straight one, the quality of the fit is essentially unaltered but the value of β is raised (Table 2). In what follows we will use values from 0·342 to 0·35 for the exponent β.

$\partial\mu/\partial\rho \sim \Gamma'^{-1}|\Delta T|^{\gamma'}$ or along the critical isochore, $\partial\mu/\partial\rho \sim \Gamma^{-1}|\Delta T|^{\gamma}$. Scaling implies that the exponents γ and γ' are equal. An estimate of these exponents for steam is obtained from PVT data. We have used two sources of data. One is a collection of precise liquid isotherms measured by Smith, Keyes and Gerry [32]. We have numerically extrapolated the data between 300 and 360°C to the vapor pressures directly measured by the same authors. The coexistence volumes so obtained agree well with those of Eck in the range of overlap. From these volumes and the limiting slopes the values of $\partial\mu/\partial\rho$ were calculated. The results, reduced by $P_c V_c$, are summarized in Table 4 and plotted in Fig. 4.

The second source of data are the PVT data of Rivkin and coworkers, reported between 1962 and 1966 [33] and discussed more fully in Section 8. After some preliminary sifting of the data, four point interpolations for equally and finally spaced densities were performed along each isotherm. From the pressure differences across the critical

isochore, $\partial\mu/\partial\rho$ was calculated. Below T_c, the data were extrapolated to the vapor pressure data of OSG [30] or to Eck's coexistence curve [23] and the limiting slope was obtained numerically. Because of a number of discrepancies among the three sets of data in the region near the critical point, the resulting limiting slopes are beset with large errors. An attempt has been made to assess these errors (Fig. 4); the data are reported in Table 4 and plotted in Fig. 4.

Above T_c, the data on the critical isochore were weighted according to their estimated error and fitted by a power law in the range 374–410°C, while T_c was varied. The fit was rather insensitive to the choice of T_c. For the most likely value, $T_c = 373{\cdot}9$°C, the results of the fit were:

$$\gamma = 1{\cdot}201 \pm 0{\cdot}006 \qquad \gamma = 1{\cdot}202 \pm 0{\cdot}008$$
$$\Gamma = 0{\cdot}0735 \pm 2\% \qquad \Gamma = 0{\cdot}0728 \pm 2\%$$
$$374\text{–}410°C \qquad 374\text{–}400°C \qquad (15)$$

Below T_c, the Keyes and Rivkin data on the liquid side from 300–373°C were combined, and fitted with a power law. The results for the fit with $T_c = 373{\cdot}9$°C are

$$\gamma'_L = 1{\cdot}09 \pm 0{\cdot}022 \qquad \gamma'_L = 1{\cdot}09 \pm 0{\cdot}026$$
$$\Gamma'_L = 0{\cdot}0329 \pm 8\% \qquad \Gamma'_L = 0{\cdot}0335 \pm 10\%$$
$$300 - 372°C \qquad 310 - 372°C \qquad (16)$$

The apparent exponent γ'_L is smaller than γ, in violation of scaling. The reason is that the $(\partial\mu/\partial\rho)_T$ data of Table 4 are not in the asymptotic range of the scaling laws. As is clear in Table 4 and Fig. 4, the $(\partial\mu/\partial\rho)_T$ symmetry between gas and liquid, which is typical of the asymptotic range, is not present in most of the range of these steam data. A similar but less pronounced deviation from symmetry has been found in other gases, such as CO_2 and Xe [19] and He^3 [15]. That the asymptotic range is small in steam below T_c may be due to the fact that the two-phase "dome" of the coexistence curve of steam is unusually wide so that even a degree below critical, the coexisting densities are far

Table 4. $(\partial\mu/\partial\rho)_T$ for steam along the coexistence curve and the critical isochore, in reduced units

Below T_c			Above T_c	
T(°C)	$(\partial\mu/\partial\rho)_{liq}$	$(\partial\mu/\partial\rho)_{gas}$	T(°C)	$(\partial\mu/\partial\rho)_T$
300	6·39		374·15	0·00172
310	5·25		374·42	0·00377
320	4·26		374·95	0·00724
330	2·99		375·01	0·00762
340	2·26		376·97	0·0186
350	1·70		378·02	0·0320
360	0·806		379·03	0·0406
			379·98	0·0526
From Smith, Keyes and Gerry [32]			379·98	0·0517
			380·99	0·0582
			382·98	0·0814
360·04	0·705	0·394	384·95	0·102
364·97	0·389		387·03	0·125
367·98	0·357	0·156	389·98	0·161
369·98	0·149		394·97	0·226
371·01		0·057		
			400·00	0·288
371·99	0·055	0·042	409·96	0·426
372·97	0·039	0·031	419·96	0·563
From Rivkin [33]			From Rivkin [33]	

from critical and perhaps outside the range of simple scaling. Above T_c, where this problem does not arise, the exponent γ is rather independent of the range and definitely nonclassical. Also, it is quite close to the values obtained for a number of other substances; 1·25, O_2 [16]; 1·17, CO_2 [34]; 1·22, CO_2 [35]; 1·18, He^3 [15].

The ratio of compressibilities above and below T_c, assuming equal slopes (Fig. 4), is about 4, a value found for many other gases as well [16, 19].

7. THE VAPOR PRESSURE OF STEAM

In equations of the van der Waals type, the vapor pressure and the pressure on the critical isochore above T_c are not analytic continuations of each other; rather, a jump occurs in the second derivative $(\partial^2 P/\partial T^2)_v$ [11, 36]. Along each of the branches, however, the pressure can be expanded as a power series in the temperature. This can no longer be expected for a nonclassical critical point. Here, one assumes a vapor pressure equation of the form [19, 2]

$$P = P_c + P_1(\Delta T) + P^- |\Delta T|^{2-\theta} + P_2(\Delta T)^2 + \ldots \tag{17}$$

with the exponent θ limited by thermodynamics [13] to

$$\theta < \alpha' + \beta. \tag{18}$$

If $\theta > 0$, (d^2P/dT^2) diverges, whereas if $\theta < 0$, this derivative increases cusplike to a finite

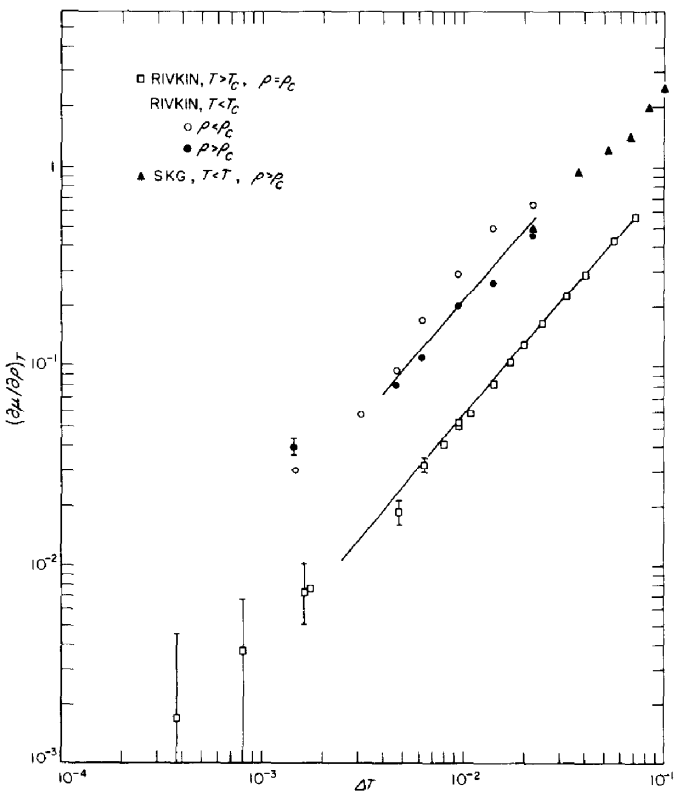

FIG. 4. Values of the compressibility $\rho^2 K_T$ derived from experimental PVT data on steam along the critical isochore (□) and along the gas (○) and liquid (●, ▲) branches of the coexistence curve. They are plotted *vs.* $|T - T_c|$ on a double logarithmic scale. The parallel straight lines indicate a $|T - T_c|^{-\gamma}$ divergence with $\gamma \sim 1{\cdot}2$.

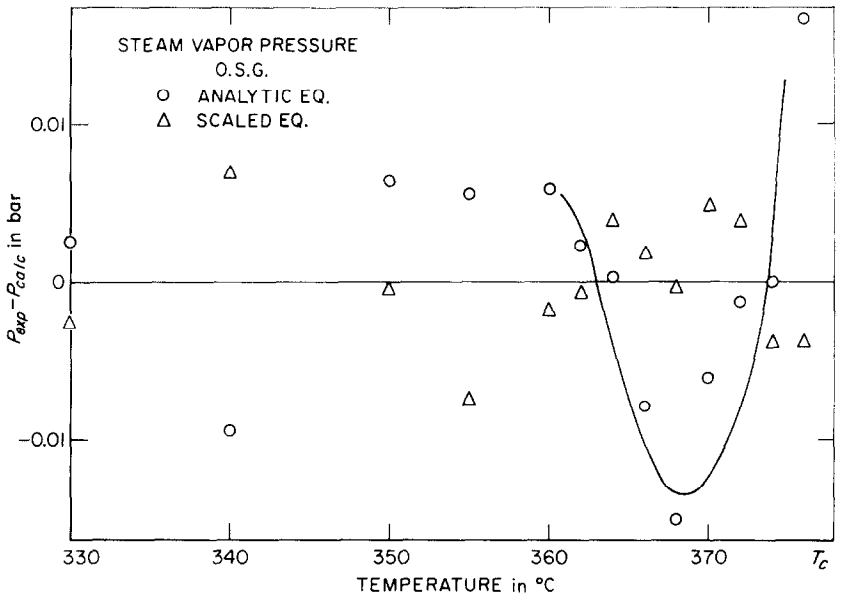

FIG. 5. Differences between vapor pressure data of steam and values calculated according to (17), Δ, and (19), ○. The solid curve connects the systematic deviations from the analytic equation (19) while the deviation from the scaled equation (17) are random.

value at T_c. The scaling laws imply that $\theta = \alpha = \alpha'$, the specific heat exponent; and also, that the critical isochore and the vapor pressure curve obey the same equation (17) but with different coefficients, P^+ and P^-, respectively, of the $|\Delta T|^{2-\theta}$ term.

The vapor pressure of steam was carefully determined by Osborne, Stimson and Ginnings

Table 5. Vapor pressure of steam, OSG [37], *and derived values of* d^2P/dT^2

Temp (°C)	Pressure (bar)	$(d^2P/dT^2)_{reduced}$ (from scaled equation (17))			$(d^2P/dT^2)_{reduced}$ (from C_v [38, 39])
		$\theta = -0.06$	$\theta = 0.06$	$\theta = 0.12$	
330	128·642	32·3	32·6	32·9	
340	146·077	35·3	35·5	35·6	33·6
350	165·367	39·2	39·2	39·1	
355	174·772	41·9	41·7	41·6	
360	186·739	45·2	45·0	45·0	45·1
362	191·288	46·9	46·7	46·7	
364	195·940	48·8	48·8	48·8	
366	200·683	51·2	51·3	51·4	
368	205·545	54·2	54·7	54·9	
370	210·524	58·4	59·5	60·1	56·7
371	213·056	61·3	63·0	63·9	
372	215·615	65·4	68·1	69·6	63·9
373	218·217	72·2	77·2	80·2	82·5
373·23			80·8	84·5	115 ± 10
373·55			89·6	94·1	128 ± 10
373·71			95·8	103·1	140 ± 10
373·79			101·6	110·6	135 ± 10

[37]. The data are reported in Table 5. Taking second differences for the highest four points, one notices immediately a marked increase when approaching T_c. This increase cannot be properly described with a classical vapor pressure equation, while a nonclassical equation of the form (17) describes the data within error. This is demonstrated in Fig. 5, where deviations from the least-squares fitted curve are displayed, using (17) with $\theta = 0{\cdot}02$ and $T_c = 373{\cdot}85°C$; and using the classical equation

$$\log P = A + \frac{B}{T} + C \log T + DT, \qquad (19)$$

which has the same number of adjustable parameters as (17). Equation (19) is incapable of following the rapid curvature near T_c. The OSG data are insensitive to the choice of T_c. Slightly better fits are obtained with negative θ's (cusp) than with positive ones, but in all cases the fit is superior to that of the analytic form. Some values of $\partial^2 P/\partial T^2$, calculated for positive and negative values of θ, are reported in Table 5.

8. THE SPECIFIC HEAT AT CONSTANT VOLUME C_v. THE EXPONENT α

In 1963, Amirkhanov and Kerimov (AK) made measurements of C_v for steam along the phase boundary [38] and in the general region of the critical point [39]. In 1968 Kerimov made more detailed measurements in the critical region, with improved temperature measurements [40]. In 1969, Amirkhanov, Stepanov and Alibekov (ASA) obtained data with an improved calorimeter along the phase boundary and in the one-phase region, but not in the critical region [41].

All measurements were made in cells of appreciable height and with the samples vigorously stirred. The effect of stirring is not known. If samples are allowed to settle without stirring near the critical point, density gradients are set up by gravity. There are contributions to the specific heat due to this redistribution of matter. These contributions have been rigorously calculated, for nonclassical equations of state, for only a few cases, such as CO_2 and Xe [42, 43] on the critical isochore. They cause an apparent deviation from asymptotic power law behavior in a temperature region near T_c. The size of this region depends on the substance, and on the height of the sample. The gravity effect in water is expected to be smaller than in most other substances. This follows from a scaling to steam of the numbers obtained for xenon [42], from which one would expect, in a cell of water 10 cm high, sizeable contributions to C_v on the critical isochore from gravity effects only for temperatures within 0·2° from T_c. These effects should be negligible not only in an unstirred but also in a stirred container if T is more than 0·2° from T_c.

ASA state that the AK boundary data were taken on a water sample contaminated by air and in a calorimeter which leaked in the critical region. They state also that the AK boundary data contain errors of calculation. The AK values of C_V on the phase boundary differ from the ASA values by 1–5 per cent. We expect therefore that the ASA boundary data are more reliable than the AK boundary data.

The AK data in the critical region are subject to the criticism of sample purity mentioned before. The 1963 data of AK and the 1968 data of Kerimov in the critical region differ by 0–10 per cent. However, the latter set of data can not be considered the more reliable. Close scrutiny of these data reveals that they are inconsistent with the OSG vapor pressure data on steam and differ in important aspects from the behavior displayed by the older data and by data on other substances. From equation (7) above we see that plots of C_v/V vs. ρ on isotherms in the two-phase region should give straight lines, the slopes of which equal $-T\mathrm{d}^2\mu/\mathrm{d}T^2$. These slopes should vary only slowly if our assumption of the analyticity of $\mathrm{d}^2\mu/\mathrm{d}T^2$ (Section 3) is correct. The C_v/V vs. ρ data for Ar, He^3 and He^4 [15, 19] indeed show this behavior. When the data for steam are considered, the ASA phase boundary data and AK critical region data indicate a rather constant value of $-T\mathrm{d}^2\mu/\mathrm{d}T^2$ in the range from 300 to 374°C of the order of 0·8 cal/g

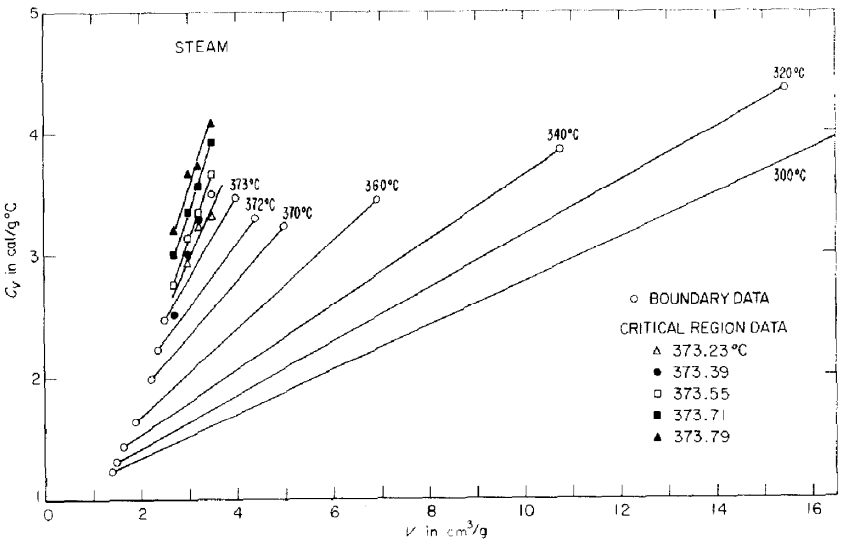

FIG. 6. Experimental values of C_v on the phase boundary [41] and in the critical region [39] of steam vs. V [38]. The increasing slope reflects the increase of d^2P/dT^2 while the intercept for $V = 0$, related to $d^2\mu/dT^2$, remains more steady.

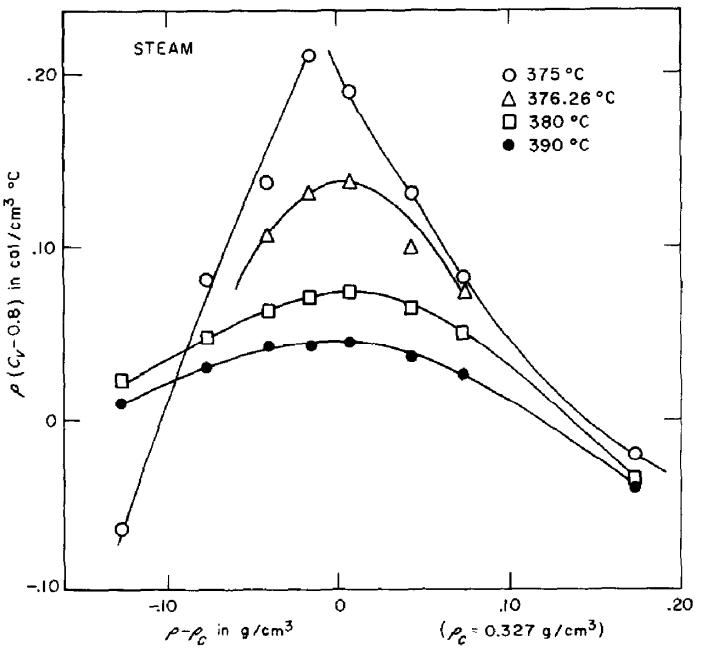

FIG. 7. Symmetrized values of the constant volume heat capacity density of steam in the supercritical region.

°C or 3350 J/kg°C. However, the 1968 Kerimov data show $-T\mathrm{d}^2\mu/\mathrm{d}T^2$ *increasing* as T_c is approached. Conversely, one can plot C_v vs. V, the slopes now being equal to $T\mathrm{d}^2P/\mathrm{d}T^2$. This is done for the AK and ASA data in Fig. 6. One notes a marked increase of the slope when the critical point is approached. However, the newer data show a *decrease* of the slope, in disagreement

In the two-phase region, the addition of the quantity $\rho T\mathrm{d}^2\mu/\mathrm{d}T^2$, with $-T\mathrm{d}^2\mu/\mathrm{d}T^2 = 0{\cdot}8$ cal/g°C, to all C_v/V data causes the two-phase data to coalesce on a single curve. In the one-phase region, an estimate of $T\mathrm{d}^2\mu/\mathrm{d}T^2$ is obtained by symmetrizing the C_v/V vs. ρ data, as described in Section 3, by subtracting a part linear in the density. AK maintain that $\rho_c = 0{\cdot}310$

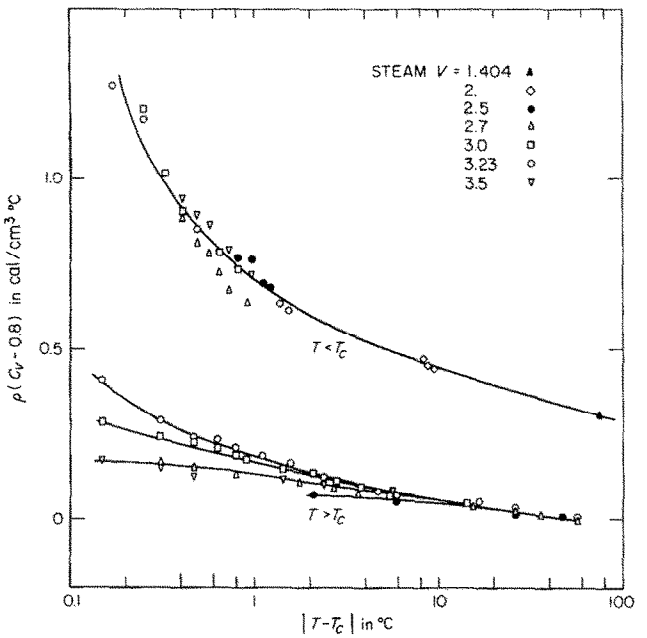

FIG. 8. Symmetrized values of the constant volume heat capacity density of steam along the critical isochore in the two-phase region (upper curve) and along several isochores in the one-phase region (lower curve) plotted vs. $|T - T_c|$ on a semilog scale. The curvature of the critical isochore data indicates a divergence faster than logarithmic.

not just with the behavior of other substances but also with the directly observed vapor pressure curve of steam (Section 7). Values for $\mathrm{d}^2P/\mathrm{d}T^2$ derived from the older C_v data are in reasonable agreement with those derived from the vapor pressure, (Table 5), but the newer data deviate by as much as a factor 2. Therefore, despite reservations about the quality of the AK data, they have to be preferred over the newer data.

The power law analysis of C_v then proceeds as described in Section 3, the Appendix, and [19].

g/cm³. However, we have found that C_v/V isotherms above T_C can be readily symmetrized only if it is assumed that ρ_c is larger, about 0·327 g/cm³. This is somewhat larger than, but reasonably close to, values of ρ_c obtained from the antisymmetry of μ–ρ isotherms, $\rho_c = 0{\cdot}3222$ g/cm³ (see Section 9), and from the coexistence curve, $\rho_c = 0{\cdot}324$ (see Section 5). The slope $-T(\partial^2\mu_C/\mathrm{d}T^2)$ is virtually independent of temperature, and equals about 0·80 cal/g °C, just as below T_C. In the lattice gas, it would equal the perfect gas specific heat, but the perfect gas

specific heat of steam is 0·37 cal/g °C at these temperatures [44]. The symmetrized specific heat is plotted in Fig. 7. Only a few points very near T_c are off the symmetric curves.

Next, the quantity $C_v/V + \rho T(\partial^2\mu/\partial T^2)$ is plotted versus $|T - T_c|$ on a semilog scale, Fig. 8. T_c is taken to be 374·20°C and is consistent with varying function of T (Appendix). This freedom is used to obtain two lines as straight and as parallel as possible. Adding 0·8 cal/cm³°C to all data produces straight parallel lines in a range of about 10°C from critical, and with slope $\alpha = 0{\cdot}9$. A slight residual curvature seems to be present in the last few tenths °C below critical. It does

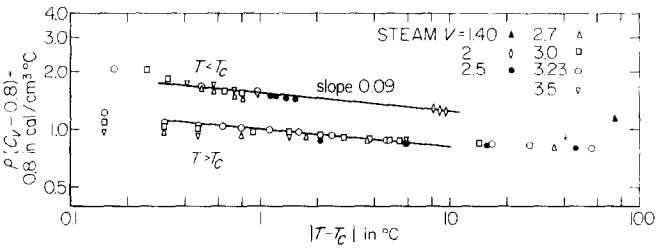

FIG. 9. Symmetrized constant volume heat capacity density of steam corrected with a constant background term, and plotted vs. $|T - T_c|$ on a double logarithmic scale. The two parallel straight lines with slopes 0·09 indicate a divergence of the type $C_v \sim t^{-\alpha}$, with $a = 0{\cdot}09$.

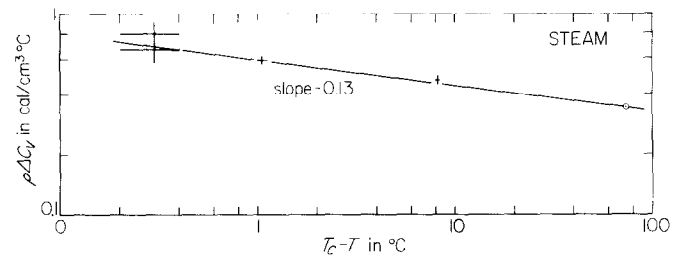

FIG. 10. Some data for the jump in the constant volume heat capacity density across the phase boundary, plotted vs. $T_c - T$ on a double logarithmic scale. The specific heat jump appears to diverge like the specific heat itself.

the highest temperature (374·11°C) at which the jump in C_v was observed. One expects a single curve for the data below T_c (upper curve); according to scaling, isochores above T_c behave like the critical isochore as long as $T - T_c$ is large but diverge from it when the critical point is approached (Appendix). Both the data in the two-phase region and along the critical isochore show marked deviations from straight lines, indicating that C_v diverges faster than logarithmically.

To obtain a power law exponent, the data are now plotted on a double log scale, Fig. 9. The scaling laws permit adding a constant or slowly not seem useful to speculate about its significance in view of the unknown effects of stirring and gravity in this range.

The jump in C_v/V when crossing the phase boundary is expected to diverge as C_v/V itself [2]. From the AK data we have calculated some of these jumps, estimated their error, and plotted them as function of $T - T_c$ in Fig. 10. It is seen that the slope of this curve equals 0·13 with a large error, but in agreement with our previous estimate of α.

Concluding, the specific heat of steam seems to diverge with about the same exponent as found for other substances [5, 7, 15, 19], thus

corroborating the nonanalytic nature of the critical point behavior.

9. SCALING OF THE STEAM *PVT* DATA

As explained in Section 4, the scaling laws for the critical region of gases imply that $\Delta\mu = \mu(\rho, T) - \mu(\rho_c\, T)$ divided by $|\Delta\rho|^{\delta}$ is a function of one parameter, the scaled temperature $x = \Delta T/|\Delta\rho|^{1/\beta}$. For testing the validity of the scaling hypothesis, we have used the large body of *PVT* data obtained by Rivkin and co-workers between 1962 and 1966 [33]. The 1966 data have to be considered superior to the older data in the region close to the critical point because much longer equilibrium times were used. The scaling of the data proceeds in several steps. First, we have interpolated in the original *PVT* data along isotherms for equal density steps, small enough (0·005 g/cm^3) to permit using the trapezoidal rule for integrating. Four-point interpolation turned out to be adequate in most cases. The integration $\mu_2 - \mu_1 = \int_1^2 V\mathrm{d}P$ was then carried out on the interpolated data. The resulting isothermal μ–ρ curves, with arbitrary zero-points for μ, were studied for antisymmetry. This property is less pronounced and extends over smaller density ranges for steam than for other substances studied [15, 16, 19]. The point of antisymmetry varied in a random way from isotherm to isotherm; a value of $\rho_c = 0{\cdot}3222$ g/cm^3 was about the best average obtainable. The μ value corresponding to this density was interpolated on each isotherm and used as the reference point. Finally, tables of $\Delta\mu$, $\Delta\rho$ were prepared for about 19 isotherms in the range 374–420°C. Several isotherms had to be rejected because there were not sufficient data to permit interpolation; others were not considered because they had been superseded by later superior data. For scaling, we have used isotherms between T_c and 420°C. Of the 1962 and 1963 data, we have rejected the 374·15°C and 374·95°C isotherms because they were remeasured in 1966. For the 400°C isotherm, we combined the 1962 and 1963 data. The other 1962 and 1963 data between 374·95°C and 419·96°C were all used. For the 1964 data, the 375·97°C and 376·97°C isotherms require some reservation because of wide spacing near the critical density. We combined the three parts of the 374·15°C isotherm taken in 1966 and used, in addition, the 374·42°C and 374·98°C isotherms reported in that year.

In view of the width of the "dome" of the coexistence curve, isotherms below T_c rarely have any points at all within the ± 25 per cent range around ρ_c. For the time being, these have not been included in our analysis.

Once the data had been sifted and the μ–ρ relation obtained, we proceeded to scale. For the parameter β we used the value 0·35 which optimizes the fit to the Eck data (Section 5) and the value 0·3426 which is the best compromise between the Eck and the OSG data (Section 5). We then made computer plots, in various ranges of x, of the quantity $|\Delta\mu|/|\Delta\rho|^{\delta}$ vs. x for various choices of T_c and δ. On inspection, good coincidence of the data on a single curve was obtained for the following T_c, δ choices

$\beta = 0{\cdot}35$	$\beta = 0{\cdot}3426$	$\beta = 0{\cdot}3426$
$T_c = 373{\cdot}90$°C	$T_c = 373{\cdot}85$°C	$T_c = 373{\cdot}95$°C
$\delta = 4{\cdot}4$	$\delta = 4{\cdot}5$	$\delta = 4{\cdot}3$
$(\gamma = 1{\cdot}16)$	$(\gamma = 1{\cdot}20)$	$(\gamma = 1{\cdot}13)$.

In order to develop a more acute test than visual inspection, we have also fitted the steam data, using the method of least-squares, to a function proposed by Missoni, Sengers and Green [19] and used successfully for a number of gases:

$$h(x) = E_1\left(\frac{x + x_0}{x_0}\right)\left[1 + E_2\left(\frac{x + x_0}{x_0}\right)^{2\beta}\right]^{(\gamma-1)/2\beta} \tag{20}$$

where E_1, E_2 are adjustable constants and $-x_0$ is the value of x at coexistence. Although the errors in interpolated $\Delta\mu$, $\Delta\rho$, and ΔT data cannot be considered completely random and uncorrelated, we have, for lack of a better procedure, tried to assign weights based on experimental error, as explained in [19], assuming

errors of 0·01°C in temperature, 0·0005 in reduced density and 0·001 in reduced chemical potential $\Delta\mu/(P_cV_c)$. If these error estimates are realistic, the standard deviation of the fit to the proper model function would be unity. Using all the data within 25 per cent from the critical density, we found, for the optimum parameter combination, standard deviations of order 3, while the high and low density ends of several isotherms were out by many times their estimated error, reflecting lack of antisymmetry. Rejecting these points did not alter the parameters significantly, but it did bring the standard deviation down to about 1·5 for optimum parameter combinations. Only a shallow minimum is obtained with respect to T_c when T_c is varied in steps of 0·05 °C. This minimum does, however, occur below 374°C. On varying δ in steps of 0·1, a pronounced minimum is obtained, so that δ is determined to $\pm 0{\cdot}1$. Some typical parameter combinations, resulting in standard deviations close to 1·5, are

$\beta = 0{\cdot}35$	$\beta = 0{\cdot}35$	$\beta = 0{\cdot}3426$
$\delta = 4{\cdot}6$	$\delta = 4{\cdot}5$	$\delta = 4{\cdot}6$
$(\gamma = 1{\cdot}23)$	$(\gamma = 1{\cdot}225)$	$(\gamma = 1{\cdot}233)$
$T_c = 373{\cdot}85$°C	$T_c = 373{\cdot}90$°C	$T_c = 373{\cdot}85$°C

From the values of E_1, E_2, β, δ and x_0, the coefficients Γ, Γ', B and D in the power law expressions

$$K_T = \Gamma|\Delta T|^{-\gamma},\ T > T_c$$
$$K_T = \Gamma'|\Delta T|^{-\gamma'},\ T < T_c$$
$$\Delta\rho = B|\Delta T|^{\beta},\ \text{coex. curve} \qquad (21)$$
$$\Delta\mu = D|\Delta\rho|^{\delta},\ T = T_c$$

were derived. For two of the above parameter sets, the values are listed in Table 6.

The coefficient Γ obtained from scaling can be compared with that derived from direct analysis of K_T along the critical isochore (Section 6). The slight difference is explained entirely by the small difference between the exponents used.

A more severe test is the value of the coefficient of the specific heat anomaly across the phase boundary; the specific heat data were taken independently from the PVT data. Taking the experimental values of the jump at 10° and 1° from critical, and assuming $\alpha = 0{\cdot}08$ as an average corresponding to our fits of the PVT data in Table 6, we obtain, for the coefficients of the jump, 40·5 at 10° and 44·0 at 1° from critical. Our fit predicts 36·5 (Table 6). We consider the agreement reasonable. It could be improved by choice of a slightly higher value of α.

Table 6. Two typical fits, and derived values of exponents and coefficients, of the equation of state of steam

T_c	373·90°C	373·85°C
β	0·35	0·3426
x_0	0·100	0·097
δ	4·5	4·6
γ	1·225	1·23336
α	0·075	0·08144
E_1	1·2346	1·2921
E_2	0·3515	0·2915
Γ	0·06752	0·06628
Γ'	0·01689	0·01492
Γ/Γ'	3·9986	4·4418
$\Delta(C_v/V)$	36·356	36·699
Δ	1·3601	1·4098

This would correspond to a decrease in the coefficients obtained from the observed C_v while it would probably increase our predicted value, as can be inferred from Table 6. The values obtained for the exponents and for the coefficients E_2, Γ, and Γ', and that of the jump in C_v/V are all very close to those obtained previously for CO_2 and Xe [19]. Substantial differences with these gases arise in the values of x_0, E_1 and Δ found for steam.

10. CONCLUSIONS

Methods developed for analyzing critical anomalies and for describing the equation of state in nonpolar gases have been applied to steam. The critical anomalies in steam have been shown to be basically the same as those in nonpolar gases. For the critical exponents, estimates of $0{\cdot}347 \pm 0{\cdot}005$ for β, $1{\cdot}20 \pm 0{\cdot}05$ for γ, $0{\cdot}1 \pm 0{\cdot}05$ for α and $4{\cdot}5 \pm 0{\cdot}1$ for δ have been obtained.

These values are all within the range of those reported for other gases [5–7, 16–19, 34, 35]. The character of the critical region of steam is therefore definitely nonclassical. The long-range effects of the dipole interaction are apparently cancelled by rapid rotation of the dipole or by other statistical averaging effects. The equation of state of steam can be scaled. Differences between critical region properties of steam and those of other gases are the low value of the coexistence curve parameter x_0 (corresponding with a wide "dome" of the coexistence curve); the small value of the critical isotherm coefficient D; the narrowness of the density range in which the μ–ρ data are anti-symmetric; and the large value of the slope of the diameter of the coexistence curve. These differences, however, are of a quantitative nature. The quality of the critical region anomalies is no different than is that of other simple gases, in spite of the somewhat longer range of the intermolecular forces. The best values we obtain for the critical parameters ρ_c and T_c vary from experiment to experiment. The values of ρ_c we obtain span a range of 0·322–0·327, higher than used in recent steam correlation. The values of T_c vary between 373·85 and 374·35; for the experiments [22, 30] with good purity control, however, the optimum T_s is close to that observed by Blank, 373·91°C [31].

ACKNOWLEDGEMENTS

This research was supported in part by the Office of National Standard Reference Data.

The authors have profited from discussions with Dr. M. Vicentini-Missoni and with Dr. M. S. Green.

REFERENCES

1. R. W. BAIN, *N.E.L. Steam Tables 1964*. Her Majesty's Stationery Office, Edinburgh (1964).
2. M. E. FISHER, Correlation functions and the critical region of simple fluids, *J. Math. Phys.* **5**, 944–962 (1964); Notes, definitions, and formulas for critical point singularities, *Critical Phenomena: Proceedings of a Conference*, edited by M. S. GREEN and J. V. SENGERS, pp. 21–26. National Bureau of Standards Miscellaneous Publication 273, Washington (1966).
3. J. J. VAN LAAR, The variability of the quantity b in van der Waals' equation of state, also in connection with the critical quantities, *Proc. Sect. Sci. K. Ned. Akad. Wet.* **14**[I], 428–442 (1911); On the value of some differential quotients in the critical point, in connection with the coexisting phases in the neighborhood of that point and with the form of the equation of state, *Proc. Sect. Sci. K. Ned. Akad. Wet.* **14**[II], 1091–1106 (1912).
4. J. E. VERSCHAFFELT, Measurements on capillary ascension of liquified carbonic acid near the critical temperature, *Communs Kamerlingh Onnes Lab* No. 28, (1896); On the critical isothermal line and the densities of saturated vapour in isopentane and carbon dioxide, *Communs Kamerlingh Onnes Lab* No. 55 (1900). D. A. GOLDHAMMER, Studien ueber die Theorie der uebereinstimmenden Zustaende, *Z. Phys. Chem.* **71**, 577–624 (1910).
5. M. R. MOLDOVER, Investigation of the specific heat of helium in the neighborhood of the critical point, Ph.D. Thesis, Stanford University (1966); M. R. MOLDOVER and W. A. LITTLE, The specific heat of He^3 and He^4 in the neighborhood of their critical points, *Critical Phenomena: Proceedings of a Conference*, edited by M. S. GREEN and J. V. SENGERS, pp. 79–85. National Bureau of Standards Miscellaneous Publication 273, Washington (1966). F. GASPARINI and M. R. MOLDOVER, Specific heat of He^3–He^4 mixtures very near the λ-line, *Phys. Rev.* **23**, 749–752 (1969).
6. A. V. VORONEL', YU. R. CHASHKIN, V. A. POPOV and V. G. SIMKIN, Measurements of the specific heat C_v of oxygen near the critical point, *Sov. Phys. JETP* **18**, 568–569 (1964). A. V. VORONEL', V. G. SNIGIREV, and YU. R. CHASHKIN, Behavior of the specific heat C_v of pure substances near the critical point, *Sov. Phys. JETP* **21**, 653–655 (1965).
7. C. EDWARDS, J. A. LIPA and M. J. BUCKINGHAM, Specific heat of xenon near the critical point, *Phys. Rev. Lett.* **20**, 496–499 (1968). J. A. LIPA, C. EDWARDS and M. J. BUCKINGHAM, Precision measurement of the specific heat of CO_2 near the critical point, *Phys. Rev. Lett.* **25**, 1086–1090 (1970).
8. M. KAC, G. E. UHLENBECK and P. C. HEMMER, On the van der Waals theory of the vapor–liquid equilibrium. I. Discussion of a one-dimensional model, *J. Math. Phys.* **4**, 216–228 (1963).
9. T. D. LEE and C. N. YANG, Statistical theory of equations of state and phase transitions. II. Lattice gas and Ising model, *Phys. Rev.* **87**, 410–419 (1952).
10. H. D. BAEHR, Der Verhalten der spezifischen Waermekapazita et C_v und der Entropie am kritischen Punkt des Wassers, *Brennst.-Waerme-Kraft* **15**, 514–522 (1963); Der Verlauf des Grenzvolume und des Dampfdrucks am kritischen Punkt des Wassers, *Forsch. Geb. Ing Wes.* **29**, 143–146 (1963).
11. J. M. H. LEVELT SENGERS, Scaling predictions for thermodynamic anomalies near the gas–liquid critical point, *I/EC Fundamentals* **9**, 470–480 (1970).
12. H. E. STANLEY, *Introduction to Phase Transitions and Critical Phenomena*, Chap. 9, Oxford University Press, New York (1971). A. J. GUTTMAN, C. J. THOMPSON and B. W. NINHAM, Determination of critical behaviour from series expansions in lattice statistics: IV. *J. Phys. C: Solid St. Phys.* **3**, 1641–1651 (1970).
13. R. B. GRIFFITHS, Ferromagnets and simple fluids near the critical point: some thermodynamic inequalities,

J. Chem. Phys. **43**, 1958–1968 (1965); G. S. RUSHBROOKE, On the thermodynamics of the critical region for the Ising problem, *J. Chem. Phys.* **39**, 842–843 (1963).
14. B. WIDOM and O. K. RICE, Critical isotherm and the equation of state of liquid–vapor systems, *J. Chem. Phys.* **23**, 1250–1255 (1955).
15. B. WALLACE, JR. and H. MEYER, Equation of state of He^3 close to the critical point, *Phys. Rev.* **A2**, 1563–1575 (1970); Critical isotherm of He^3, *Phys. Rev.* **A2**, 1610–1612 (1970). H. MEYER, Private communication (1971).
16. L. A. WEBER, Density and compressibility of oxygen in the critical region, *Phys. Rev.* **A2**, 2379–2388 (1970).
17. C. J. PINGS and R. K. TEAGUE, Experimental study of the shape of the coexistence curve of argon near the critical state, *Phys. Lett.* **26A**, 496–497 (1968).
18. J. M. H. LEVELT SENGERS, J. STRAUB and M. VICENTINI-MISSONI, Coexistence curves of CO_2, N_2O, $CClF_3$ in the critical region, *J. Chem. Phys.* **54**, 5034–5050 (1971).
19. M. VICENTINI-MISSONI, J. M. H. LEVELT SENGERS and M. S. GREEN, Scaling analysis of thermodynamic properties in the critical region of fluids, *J. Res. Natn. Bur. Stand.* **73A**, 563–583 (1969).
20. C. N. YANG and C. P. YANG, Critical point in liquid-gas transitions, *Phys. Rev. Lett.* **13**, 303–305 (1964).
21. B. WIDOM, Equation of state in the neighborhood of the critical point, *J. Chem. Phys.* **43**, 3898–3905 (1965).
22. R. B. GRIFFITHS, Thermodynamic functions for fluids and ferromagnets near the critical point, *Phys. Rev.* **158**, 176–187 (1967).
23. H. ECK, Untersuchungen im Saettigungzustand des Wassers von 350°C bis zur kritischen Temperatur, *Phys. Z.* **40**, 3–15 (1939).
24. E. S. NOWAK, R. J. GROSH and P. E. LILEY, A survey of PVT data for water in the critical region, *J. Heat Transfer* **83C**, 1–13 (1961); Smoothed pressure-volume-temperature data for water in the critical region derived from experimental measurements, *J. Heat Transfer* **83C**, 14–26 (1961).
25. E. SCHMIDT, *VDI-Wasserdampftafeln*. Springer-Verlag, Berlin (1963).
26. *E.R.A. 1967 Steam Tables*. St. Martin's Press, New York (1967).
27. N. D. MERMIN and J. J. REHR, Generality of the singular diameter of the liquid-vapor coexistence curve, *Phys. Rev. Lett.* **26**, 1155–1156 (1971).
28. J. ZOLLWEG and B. WIDOM, private communication (1971).
29. M. E. FISHER and P. E. SCESNEY, Visibility of critical-exponent renormalization, *Phys. Rev.* **A2**, 825–835 (1970).
30. N. S. OSBORNE, H. F. STIMSON and D. C. GINNINGS, Calorimetric determination of the thermodynamic properties of saturated water in both the liquid and gaseous states from 100 to 374°C, *J. Res. Natn. Bur. Stand.* **18**, 389–447 (1937).
31. G. BLANK, Neue Bestimmung des kritischen Punktes von leichtem und schwerem Wasser, *Warme-Stoffuebertragung* **2**, 53–59 (1969).
32. L. B. SMITH, F. G. KEYES and H. T. GERRY, The vapor pressure of water, *Proc. Am. Acad. Arts Sci.* **69**, 137–168 (1934). L. B. SMITH and F. G. KEYES, The volumes of unit mass of liquid water and their correlation as a function of pressure and temperature, *Proc. Am. Acad. Arts Sci.* **69**, 285–312 (1934).
33. S. L. RIVKIN and T. S. AKHUNDOV, Experimental investigation of the specific volume of water, *Teploenergetika* **9** (1), 57–65 (1962); Experimental determination of the specific volume of water at temperatures in the range 374·15–500°C and pressures up to 600 kg/cm², *Teploenergetika* **10** (9) 66–71 (1963), S. L. RIVKIN and G. V. TROIANOVSKAIA, Determination of the specific volume near the critical region, *Teploenergetika* **11** (10), 72–75 (1964). S. L. RIVKIN, T. S. AKHUNDOV, E. K. KREMNEVSKAIA and N. N. ASSADULAIEVA, A study of the specific volumes of water in the region close to the critical point, *Teploenergetika* **13** (4), 59–62 (1966). S. L. RIVKIN, Private communication (1968). [Teploenergetika is translated as Thermal Engineering.]
34. J. A. WHITE and B. S. MACCABEE, Temperature dependence of critical opalescence in carbon dioxide, *Phys. Rev. Lett.* **26**, 1468–1471 (1971). B. S. MACCABEE and J. A. WHITE, Temperature variation of the correlation length of carbon dioxide at its critical density, *Phys. Lett.* **35A**, 187–188 (1971).
35. JOSEPH H. LUNACEK and DAVID S. CANNELL, Long-range correlation length and isothermal compressibility of carbon dioxide near the critical point, *Phys. Rev. Lett.* **27**, 841–844 (1971).
36. R. E. BARIEAU, Discontinuities in some thermodynamic quantities at the critical point of an analytic fluid, *J. Chem. Phys.* **49**, 2279–2282 (1968).
37. N. S. OSBORNE, H. F. STIMSON, E. F. FIOCK and D. C. GINNINGS, The pressure of saturated water vapor in the range 100°–374°C, *J. Res. Natn. Bur. Stand.* **10**, 155–188 (1933).
38. KH. I. AMIRKHANOV and A. M. KERIMOV, Investigation of the heat capacity C_v of water and water vapor by the direct method along the saturation curve including the critical point, *Teploenergetika* **10** (8), 64–69 (1963).
39. KH. I. AMIRKHANOV and A. M. KERIMOV, Experimental investigation of the heat capacity C_v of water and water vapor at supercritical parameters of state, *Teploenergetika* **10** (9), 61–65 (1963).
40. A. M. KERIMOV, Investigation of the isochoric specific heat of water and steam near the critical point, *Teploenergetika* **15** (1), 60–65 (1968).
41. KH. I. AMIRKHANOV, G. V. STEPANOV and B. G. ALIBEKOV, *Isochoric Heat Capacity of Water and Steam*. Dagestansk Branch of the USSR Academy of Sciences, Makhachkala (1969).
42. H. SCHMIDT, Critical region scaled equation-of-state calculations and gravity effects, *J. Chem. Phys.* **54** 3610–3621 (1971).
43. M. BARMATZ and P. C. HOHENBERG, Test of a parametric equation of state and calculation of gravity effects at the gas–liquid critical point, *Phys. Rev. Lett.* **24**, 1225–1229 (1970).
44. A. S. FRIEDMAN and L. HAAR, High speed machine computation of ideal gas thermodynamic functions. I. Isotopic water molecules, *J. Chem. Phys.* **22**, 2051–2058 (1954).

APPENDIX

Griffiths, in a recent paper [22], has presented a treatment of the thermodynamics near critical points in the scaling-law description. A brief summary for the gas–liquid case follows here.

The basic equation is that for the reduced chemical potential difference $\Delta\mu = [\mu(\rho, T) - \mu(\rho_c, T)]/P_cV_c$ in terms of the reduced density difference $\Delta\rho = (\rho - \rho_c)/\rho_c$ and the reduced temperature difference $t = (T - T_c)/T_c$:

$$\Delta\mu = \Delta\rho|\Delta\rho|^{\delta-1}h(x) \tag{A.1}$$

$$\text{with } x = t/|\Delta\rho|^{1/\beta}$$

and $h(x)$ analytic in the range $-x_0 < x < \infty$; $h(x) = 0$ at $x = -x_0$, which defines the coexistence curve

$$|\Delta\rho| = x_0^{-\beta}|t|^{\beta}. \tag{A.2}$$

Analyticity of $h(x)$ implies that for x near 0,

$$h(x) = \sum_{j=0}^{\infty} h_j x^j, \tag{A.3}$$

so that the critical isotherm is given by

$$|\Delta\mu| = h_0|\Delta\rho|^{\delta}. \tag{A.4}$$

It is desirable that $\Delta\mu$ be analytic near the critical isochore, since higher order phase transitions are not expected there. Thus

$$\Delta\mu = \sum_{n=1}^{\infty} f_n(t)(\Delta\rho)^{2n-1} \tag{A.5}$$

for small $\Delta\rho$.

This, combined with (A.1) and (A.2), implies the following expansion for $h(x)$ at large x (small $\Delta\rho$):

$$h(x) = \sum_{n=1}^{\infty} \eta_n x^{\beta(\delta+1-2n)} \tag{A.6}$$

From this it readily follows that the compressibility, inversely proportional to $(\partial\mu/\partial\rho)_T$, must vary as $t^{-\beta(\delta-1)} = t^{-\gamma}$ along the critical isochore.

For a complete thermodynamic description the Helmholtz free energy per unit volume $a = A/V$, as function of the variables ρ and T, is needed. Other thermodynamic functions, such as the chemical potential μ, the entropy per unit volume s, the pressure p and the specific heat per unit volume C_v/V then follow:

$$\mu = (\partial a/\partial\rho)_T \tag{A.7}$$

$$s = -(\partial a/\partial T)_\rho \tag{A.8}$$

$$P = \mu\rho - a \tag{A.9}$$

$$C_v/V = -T(\partial^2 a/\partial T^2)_\rho . \tag{A.10}$$

According to (A.7), the expression for a can be obtained from μ by integration with respect to density. It will contain two unspecified functions of temperature; since the scaled equation (A.1) describes only the difference $\Delta\mu$, $\mu_s = \mu(\rho_c, T)$ will be one temperature function yet unspecified. In the free energy it will occur multiplied by the density. It is assumed to behave analytically. This is true for the Ising model but not certain for real systems. In integrating μ with respect to ρ, another unspecified function of the temperature, $A_0(T)$, independent of the density, will appear in a.

Griffiths has shown that for the general case, $\alpha = 2 - \beta(\delta + 1)$ between 0 and 1, $a(\Delta\rho, T)$ can be written as

$$a(\Delta\rho, T) = A_0(T) + |\Delta\rho|^{\delta+1} a_\alpha(x) + \mu_c\rho, \tag{A.11}$$

where $a_\alpha(x)$ is related to $h(x)$ through the differential equation

$$-xa'_\alpha(x) + (2 - \alpha)\, a_\alpha(x) = \beta h(x) \tag{A.12}$$

and $A_0(T)$ is an analytic function of temperature; $a_\alpha(x)$ possesses a power series expansion in x for small x whereas for $x \to \infty$, it can be expanded as

$$a_\alpha(x) = Cx^{2-\alpha} + \tfrac{1}{2}\sum_{n=1}^{\infty} n^{-1}\eta_n x^{2-\alpha-2\beta n}. \tag{A.13}$$

It is the first term that causes the specific heat to diverge as $t^{-\alpha}$ on the critical isochore, and to behave as $t^{-\alpha}$ on all isochores when x is large.

The scaled expression for the specific heat C_v is

$$C_v/VT = -P_c(\mathrm{d}^2A_0(T)/\mathrm{d}T^2) - P_cT_c^{-2}|\Delta\rho|^{-\alpha/\beta}a''_\alpha(x) - \rho(\mathrm{d}^2\mu_c/\mathrm{d}T^2), \tag{A.14}$$

the first two terms on the right-hand side being symmetric in $\Delta\rho$, the third one linear in ρ. These properties have been used in Sec. 8.

For the pressure we have

$$P/P_c = |\Delta\rho|^{\delta+1}\{h(x) - a_\alpha(x)\} - A_0(T) + |\Delta\rho|\ (\Delta\rho)\, h\alpha), \tag{A.15}$$

where the first two terms are symmetric in $\Delta\rho$, the third one antisymmetric.

ANOMALIES THERMODYNAMIQUES PRES DU POINT CRITIQUE DE LA VAPEUR

Résumé—Des idées sur le caractère des anomalies critiques obtenues à partir d'un modèle de gaz en réseau sont testées sur les propriétés thermodynamiques de la vapeur, à l'aide de méthodes développées pour des gaz non polaires. On montre que les anomalies critiques dans la vapeur ne sont pas classiques mais très semblables à celles des gaz simples. Spécifiquement les exposants obtenus par l'analyse en loi-puissance de la courbe de coexistence, chaleur spécifique C_v et coefficient de compressibilité K_T sont $\beta = 0{,}347 \pm 0{,}005$, $\alpha = 0{,}1 \pm 0{,}05$, $\gamma = 1{,}20 \pm 0{,}05$ impliquant $\delta = 4{,}4^5$. Puisque le point critique est un point singulier de l'analyse du comportement thermodynamique, l'équation d'état peut être un moyen approprié de description de la région critique.[5] Quelques résultats d'une telle analyse des données P, V, T sont présentés et on montre qu'ils concordent avec des mesures indépendantes de pression de vapeur et de chaleur spécifique et avec les exposants donnés. La meilleure valeur obtenue pour la température critique par ce moyen est 373,9°C ± 0,05 tandis que des valeurs entre 322 et 327 kg/m^3 sont obtenues pour la masse volumique critique dépendant de la propriété analysée.

THERMODYNAMISCHE ANOMALIEN NAHE DEM KRITISCHEN PUNKT VON WASSERDAMPF

Zusammenfassung—Vorstellungen über den Charakter der kritischen Anomalien—abgeleitet aus dem Gittergasmodell—werden an den thermodynamischen Eigenschaften von Wasserdampf mit Methoden getestet, die für unpolare Gase entwickelt worden sind. Es wird gezeigt, dass die kritischen Anomalien bei Wasserdampf nicht von klassischer Natur sind und jenen der einfachen Gase sehr ähneln. Insbesondere ergeben sich die durch Auswertung der Potenzgesetze gewonnenen Exponenten für die Koexistenzkurve, die spezifische Wärme und die Kompressibilität zu: $\beta = 0{,}347 \pm 0{,}005$, $\alpha = 0{,}1 \pm 0{,}05$, $\gamma = 1{,}2 \pm 0{,}05$, darin ist implizit enthalten $\delta = 4{,}45$. Da der kritische Punkt damit nichtanalytisch im thermodynamischen Verhalten ist, können die normierten Zustandsgleichungen geeignet sein, den kritischen Bereich zu beschreiben Einige Ergebnisse einer solchen Analyse der PVT-Daten aus den Skalengesetzen werden vorgelegt, und es zeigt sich, dass sie konsistent sind mit unabhängig davon gemessenen Werten des Dampfdruckes und der spezifischen Wärme und mit den angegebenen Exponenten. Der beste Wert für die kritische Temperatur aus den Skalengesetzen ist 373,9°C ± 0,05, für die kritische Dichte wurden, abhängig von den untersuchten Eigenschaften, Werte zwischen 0,322 und 0,327 g/cm^3 erhalten.

ТЕРМОДИНАМИЧЕСКИЕ АНОМАЛИИ ВОЗЛЕ КРИТИЧЕСКОЙ ТОЧКИ ВОДЯНОГО ПАРА

Аннотация—Соображения о характере критических аномалий, полученных на решетчатых газовых моделях, проверялись в приложении к термодинамическим свойствам пара с помощью методов, разработанных для неполярных газов. Показано, что критические аномалии в водяном паре не носят классический характер и подобны аномалиям в простых газах. Поскольку критическая точка является точкой неаналитичности в термодинамическом случае, масштабированное состояние может быть использовано для описания критической области. Представлены некоторые результаты такого масштабированного анализа данных, и показано их соответствие с измеренным давлением пара и данными для удельной теплоемкости. Наилучшее значение, полученное для критической температуры путем масштабирования, равно 373,9°C±0,05°, а значения для критической плотности лежат в пределах от 0,322 до 0,327 г/см^3.